Acta Mech
https://doi.org/10.1007/s00707-025-04397-4

ORIGINAL PAPER

Jens Wittenburg · Attila Genda

Equilibria and stability of a rigid body suspended by a flexible string: analyzing two suspension systems

Received: 3 February 2025 / Revised: 24 March 2025 / Accepted: 18 May 2025
© The Author(s) 2025

Abstract Subject of investigation are equilibrium positions and their stability of a rigid body suspended by a massless, flexible, inextensible string of given length, the endpoints of which are attached to two points of the body. Two suspensions are investigated. In Suspension I, the string is passed over two frictionless hooks fixed on a horizontal line a given distance apart. In Suspension II, the string is passed over a frictionless pulley of given radius, the center of which is a fixed point. The center of mass is an arbitrarily given point of the body. Suspension I: Equilibrium positions for a given center of mass are determined by the positive roots of two 8^{th}-order polynomial equations. A bifurcation curve divides a body-fixed plane into domains differing in the number of equilibrium positions depending on the location of the center of mass. The total number of equilibrium positions is between four and eight, depending on the parameters of the system. Stability and instability criteria are formulated. By the results obtained, the special case of the single-hook suspension is covered. Suspension II: Every mathematical relationship describing suspension I is valid, in modified and more complex form, for suspension II.

1 Introduction

The study of suspended objects has long been a topic in theoretical mechanics, addressing both material points and rigid three-dimensional bodies. The motion of a material point suspended on a massless, inextensible string with fixed endpoints has been examined extensively in classical texts such as those by *Appell* [1] and *Levi-Civita* and *Amaldi* [2]. In particular, the case of a heavy bead constrained by a string presents a rich theoretical framework for understanding equilibrium and stability. Recent advancements have extended such studies to include material points constrained by strings interacting with rigid bodies [3–6]. These investigations have practical applications, for example, in the study of orbital tethered systems [7].

Geometrically related problems of stability with several equilibria arise in the stability of floating cranes [8], liquid-filled containers [9,10], equilibrium positions of floating bodies [11–13] and stability of tensegrity structures [14]. These problems are all related to catastrophe theory [15–17], and often lead to bifurcations of co-dimension higher than one due to the large number of geometrical parameters.

In [18,19], equilibrium positions of a body suspended by a massless, flexible, inextensible string passed over a frictionless hook was investigated, offering insights into the existence and stability of equilibrium positions. Stability conditions relate to geometric properties of the suspension system, such as string length, location of fixation points and location of the center of mass. Much of the existing research assumes idealized

J. Wittenburg · A. Genda (✉)
Institute of Engineering Mechanics, Karlsruhe Institute of Technology, Kaiserstr. 12, 76131 Karlsruhe, Germany
E-mail: attila.genda@kit.edu

J. Wittenburg
E-mail: jens.wittenburg@kit.edu

Published online: 12 June 2025

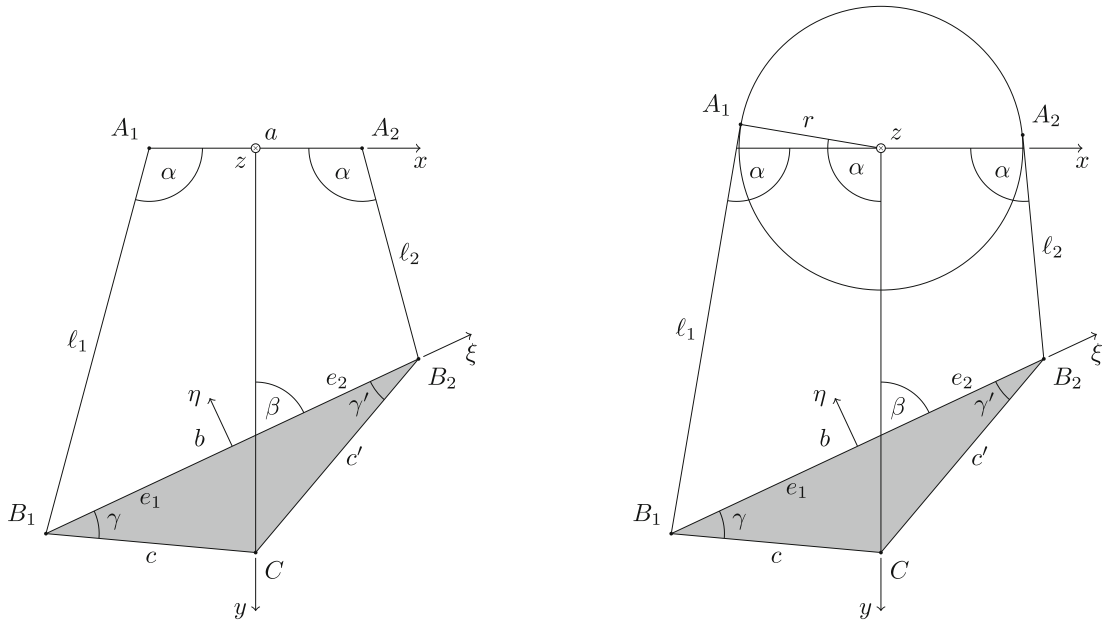

(a) Suspension I: The string is hung over $A_1 - A_2$ **(b)** Suspension II: The string is hung over a pulley

Fig. 1 Suspension problem settings. The body with center of mass C, represented by the gray triangle is suspended using a massless, flexible, inextensible string with endpoints fixed to two points B_1 and B_2 of the body

conditions, such as frictionless constraints, limiting the applicability to real-world systems. However, a recent study by *Burov* and *Nikonov* [20] analyzed the effects of dry friction resulting in non-isolated equilibrium positions distributed continuously along the suspension angle.

The current paper investigates equilibrium positions and their stability of a rigid body suspended by a massless, flexible, inextensible string with endpoints fixed to two points of the body. Two distinct suspension cases are examined:

- *Suspension I*: The string is passed over *two frictionless hooks* fixed on a horizontal line, separated by a given distance. Equilibrium positions are determined by the roots of two eighth-order polynomial equations. The bifurcation analysis reveals domains in the parameter space with varying numbers of equilibrium points, ranging from four to eight. Stability criteria for these positions are also established. This setup generalizes the simpler single-hook suspension problem.
- *Suspension II*: The string is passed over a *frictionless pulley* with a fixed center and with given radius. Every mathematical relationship describing suspension I is valid, in modified and more complex form, for suspension II.

The results extend previous work by providing a detailed characterization of equilibrium and stability under more generalized and practical suspension setups. The findings contribute to a deeper understanding of the mechanics of suspended bodies and may have implications for both theoretical studies and engineering applications.

The paper is structured as follows: In Sect. 2, the problem setting for both the double-hook and the pulley suspension cases is described. In Sect. 3, equations determining equilibrium positions and bifurcation points of Suspension I are derived. In Sect. 4, the case of the symmetric body is discussed. In Sect. 5, the special case of the single-hook suspension is treated. In Sect. 6, stability criteria are formulated for the equilibria of Suspension I. In Sect. 7, equilibrium positions of Suspension II are derived. In Sect. 8, the investigation is concluded, and the scope for future research is provided.

2 Problem setting

In Fig. 1, two suspensions I and II of a rigid body by a massless, flexible, inextensible string of given length L are shown. The body-fixed endpoints B_1, B_2 of the string are a distance b apart. In Fig. 1a (suspension I), the string is passed over two frictionless hooks A_1, A_2 which are fixed on a horizontal line a distance a apart. In Fig. 1b (suspension II), the string is passed over a frictionless pulley of radius r, the center of which is a fixed point. In both figures, the body is represented by the triangle $B_1 - B_2 - C$ with C being the center of mass defined by its distance c from B_1 and by the angle γ or, alternatively, by c' and γ'. Given are L, a, b, r, c and γ. Subjects of investigation are equilibrium positions and their stability. For Suspension II, every mathematical relationship describing Suspension I is valid in a modified and more difficult form.

Suspension I

The total length of the string is $L = \ell_1 + \ell_2 + a$. With the constant $\ell = L - a$,

$$\ell_1 + \ell_2 = \ell. \tag{1}$$

We define the non-dimensional parameters

$$p = a/b \quad \text{and} \quad q = \ell/b. \tag{2}$$

The construction requires that

$$\ell > |a - b|. \tag{3}$$

With $\ell_{1,2} \neq 0$ and a tight string, the body has five degrees of freedom. In the x, y, z-system shown in Fig. 1a with its origin at the midpoint between A_1 and A_2 and with vertical y-axis the coordinate y_C of the center of mass C is a function $y_C(q_1, \ldots, q_5)$ of five generalized coordinates. Equilibrium positions are determined by the five equations $\partial y_C/\partial q_i = 0$ ($i = 1, \ldots, 5$). Stability conditions are formulated in terms of the second-order-derivatives $\partial^2 y_C/(\partial q_i \partial q_j)$ ($i, j = 1, \ldots, 5$). In Sects. 3–5, equilibrium positions are determined by a simpler method involving a single generalized coordinate. Stability and instability conditions are the subject of Sect. 6.

3 Equilibrium positions

In a state of equilibrium with $\ell_{1,2} \neq 0$, the body is subject to its weight and to string forces acting at B_1, B_2. Since the hooks are frictionless, these string forces are equal in magnitude. Therefore, a state of (stable or unstable) equilibrium is characterized as follows. As shown in Fig. 1a, the lines $A_1 - B_1$ and $A_2 - B_2$ are under the same angle $\alpha > 0$ against the horizontal x-axis. The center of mass C is located on the y-axis. Hence, the

$$\text{equilibrium condition} \quad x_C = 0 \quad (\ell_{1,2} \neq 0). \tag{4}$$

For determining equilibrium positions, the system is treated as planar single-degree-of-freedom system with α as independent variable. In order to find all equilibrium positions, the cases $+\gamma$ and $-\gamma$ are investigated.

The reflection of an equilibrium position in the y-axis is an equilibrium position of the reflected triangle with the parameters (c', γ') instead of (c, γ). If $\ell_1 < \ell_2$ in one position, then $\ell_1 > \ell_2$ in the other. Instead of determining all equilibrium positions for the two parameter combinations $(c, \pm\gamma)$, the simpler problem is solved to determine all equilibrium positions with $\ell_1 \geq \ell_2$ for the four parameter combinations $(c, \pm\gamma)$ and $(c', \pm\gamma')$. In what follows, (c, γ) and (c', γ') is written with γ and γ' both positive and negative.

The points B_1 and B_2 in Fig. 1a have the x, y-coordinates

$$B_1 = [-a/2 + \ell_1 \cos\alpha\ ,\ \ell_1 \sin\alpha], \qquad B_2 = [a/2 - \ell_2 \cos\alpha\ ,\ \ell_2 \sin\alpha]. \tag{5}$$

In Fig. 1a, the angle β is defined:

$$\sin\beta = (x_{B_2} - x_{B_1})/b = p - q\cos\alpha. \tag{6}$$

$$\frac{\mathrm{d}}{\mathrm{d}\alpha}\sin\beta = q\sin\alpha, \quad \frac{\mathrm{d}}{\mathrm{d}\alpha}\cos\beta = -q\sin\alpha\tan\beta, \quad \frac{\mathrm{d}}{\mathrm{d}\alpha}\tan\beta = q\frac{\sin\alpha}{\cos^3\beta}. \tag{7}$$

From $(B_1 - B_2)^2 = b^2$, it follows that

$$\ell_1 - \ell_2 = b\,\frac{\cos\beta}{\sin\alpha}. \tag{8}$$

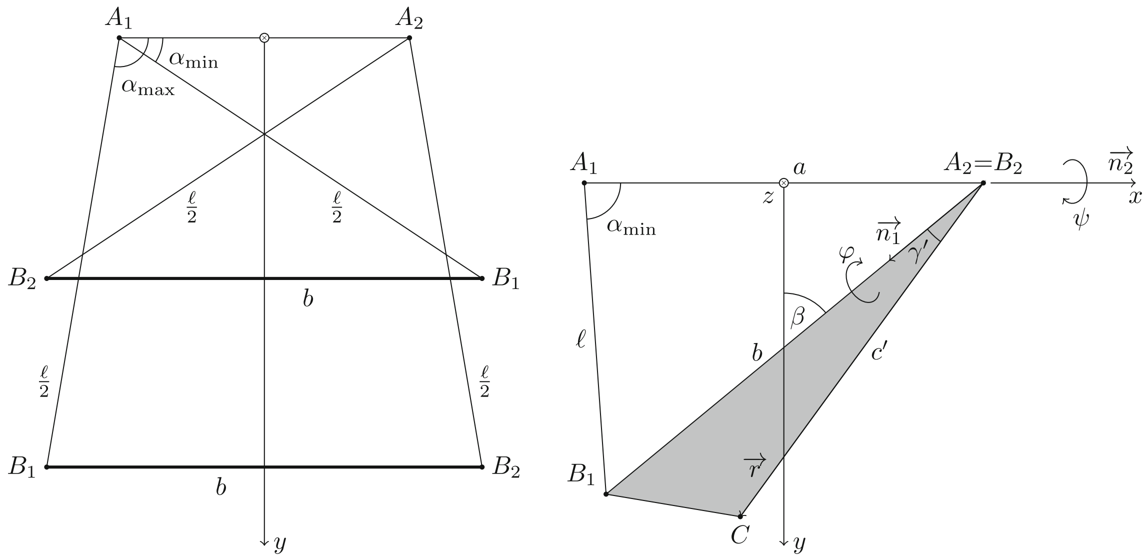

(a) $\ell > a+b$ **(b)** $\ell < a+b$

Fig. 2 Extremal angles $\alpha_{\min}$, $\alpha_{\max}$. Unit vectors $\vec{n}_1$, $\vec{n}_2$ and rotation angles φ, ψ used in Sect. 7

Hence with Eq. (1), we have

$$\ell_{1,2} = \frac{b}{2}\left(q \pm \frac{\cos\beta}{\sin\alpha}\right). \tag{9}$$

The sections e_1, e_2 of b made by the y-axis are

$$e_{1,2} = \frac{\mp x_{B_{1,2}}}{\sin\beta} = \frac{b}{2}\,(1 \mp \cot\alpha\cot\beta)\,. \tag{10}$$

Extremal angles $\alpha_{\min}$ and $\alpha_{\max}$ occur in the positions shown in Fig. 2a,b. The positions in Fig. 2a are characterized by $\sin\beta = -1$ ($\alpha = \alpha_{\min}$) and $\sin\beta = +1$ ($\alpha = \alpha_{\max}$). The definition of $\alpha_{\min}$ does not apply if the position with contact $B_2 = A_2$ is possible, i.e., if the triangle inequality $\ell < a + b$ is satisfied (Fig. 2b). The contact condition $\ell_2 = 0$ yields

$$\cos\beta/\sin\alpha_{\min} = q, \tag{11}$$

which is the sine law in the triangle (A_1, B_1, A_2) of Fig. 2b. The cosine law yields $\cos\alpha_{\min}$. The results are summarized in the formulas

$$\cos\alpha_{\min} = \begin{cases} \dfrac{p+1}{q} & (\ell > a+b), \\ \dfrac{p^2+q^2-1}{2pq} & (\ell < a+b), \end{cases} \qquad \cos\alpha_{\max} = \frac{p-1}{q}. \tag{12}$$

In Fig. 2b, a contact force $F_y \geq 0$ applied at B_2 keeps the body of weight G in equilibrium under the condition $Gx_C + F_y a/2 = 0$. Hence, the statement:

The position with contact $B_2 = A_2$ is an equilibrium position if in this position $x_C \leq 0$. (13)

3.1 Equilibrium positions with $\ell_1 \geq \ell_2 > 0$

In terms of the parameters (c, γ), the coordinates of C are

$$\left.\begin{aligned} x_C &= x_{B_1} + c\sin(\beta+\gamma) = \frac{b}{2}\left[-p + \left(q + \frac{\cos\beta}{\sin\alpha}\right)\cos\alpha\right] + c(\sin\beta\cos\gamma + \cos\beta\sin\gamma),\\ y_C &= y_{B_1} - c\cos(\beta+\gamma) = \frac{b}{2}\,(q\sin\alpha + \cos\beta) - c(\cos\beta\cos\gamma - \sin\beta\sin\gamma) \end{aligned}\right\} \tag{14}$$

and with the constants

$$\mu = 2\frac{c}{b}\cos\gamma - 1, \qquad \sigma = 2\frac{c}{b}\sin\gamma, \tag{15}$$

$$x_C = \frac{b}{2}[\mu\sin\beta + (\cot\alpha + \sigma)\cos\beta], \qquad y_C = \frac{b}{2}(q\sin\alpha + \sigma\sin\beta - \mu\cos\beta). \tag{16}$$

Consider Fig. 1a again. From the cosine law and the sine law, it follows that $\mu' = (2c'/b)\cos\gamma' - 1 = -\mu$, and $\sigma' = (2c'/b)\sin\gamma' = \sigma$. From this, it follows that the equilibrium conditions $x_C = 0$ with the four parameter combinations (c, γ) and (c', γ') (γ and γ' both positive and negative) result in the equations

$$\mu\sin\beta + (\cot\alpha \pm \sigma)\cos\beta = 0, \qquad -\mu\sin\beta + (\cot\alpha \pm \sigma)\cos\beta = 0. \tag{17}$$

No extraneous roots are introduced by squaring. Squaring and multiplying with $\sin^2\alpha$ results in the equations

$$[\mu\sin\alpha(p - q\cos\alpha)]^2 = (\cos\alpha \pm \sigma\sin\alpha)^2[1 - (p - q\cos\alpha)^2], \tag{18}$$

and with the new variable $u = \tan\alpha/2$ and with

$$v = q + p, \quad w = q - p \tag{19}$$

in the equations

$$[2\mu u(vu^2 - w)]^2 = (u^2 \pm 2\sigma u - 1)^2\,[(1 + u^2)^2 - (vu^2 - w)^2]. \tag{20}$$

Each real solution $u > 0$ of these two 8$^{\text{th}}$-order equations determines an equilibrium position. The number of equilibrium positions depends on the parameters a, b, ℓ, c and γ. This dependency is investigated in Sect. 3.2.

3.2 Lines α

Every angle α in the interval $\alpha_{\min} \leq \alpha \leq \alpha_{\max}$ determines a position of the polygon $A_1 - B_1 - B_2 - A_2$. Every position without contact $B_2 = A_2$ is an equilibrium position if the center of mass is an *arbitrary point on the body-fixed line* coinciding with the y-axis. In the body-fixed ξ, η-system shown in Fig. 1a with its origin at the midpoint between B_1 and B_2 this line, referred to as line α, has the slope $\tan\beta$. It intersects the ξ-axis at the point $b/2 - e_2$ and the η-axis at the point $(b/2)\cot\alpha$. Its equation is

$$F = -\frac{\eta}{b} + \frac{\xi}{b}\tan\beta + \frac{1}{2}\cot\alpha = 0. \tag{21}$$

In the case $\ell > a + b$, the lines $\alpha = \alpha_{\min}$ and $\alpha = \alpha_{\max}$ both coincide with the η-axis. In the case $\ell < a + b$, only the line $\alpha = \alpha_{\max}$ coincides with the η-axis.

By the manifold of lines α, a curve E is enveloped. This curve is determined by the equations $F = 0$ and $\mathrm{d}F/\mathrm{d}\alpha = 0$.

$$\frac{\mathrm{d}F}{\mathrm{d}\alpha} = \frac{\xi}{b}\,\frac{q\sin\alpha}{\cos^3\beta} - \frac{1}{2\sin^2\alpha} = 0 \tag{22}$$

yields

$$\frac{\xi}{b} = \frac{1}{2q}\left(\frac{\cos\beta}{\sin\alpha}\right)^3. \tag{23}$$

The curve E intersects the ξ-axis at the point $\xi_0 = b/2 - e_{2\min}$. With $\eta = 0$, Eqs. (21) and (23) yield for the associated angle α_0

$$\frac{1}{q\sin^3\alpha_0}(\sin\beta\cos^2\beta + q\cos\alpha_0\sin^2\alpha_0) = 0 \tag{24}$$

and with Eq. (6)

$$p - q\cos^3\alpha_0 - (p - q\cos\alpha_0)^3 = 0. \tag{25}$$

Let P_1 and P_2 be the points of tangency of E with the lines $\alpha = \alpha_{\min}$ and $\alpha = \alpha_{\max}$, respectively. Their coordinates are:

Case 1: ($\ell > a + b$)

$$\xi_{1,2} = 0, \quad \eta_{1,2} = \frac{b}{2}\frac{p \pm 1}{\sqrt{q^2 - (p \pm 1)^2}}. \tag{26}$$

Case 2: ($\ell < a + b$)

$$\begin{aligned} \xi_1 &= \frac{b}{2}q^2, \quad \eta_1 = \frac{b}{2}\left[q^2\tan\beta(\alpha_{\min}) + \cot\alpha_{\min}\right], \\ \xi_2 &= 0, \qquad \eta_2 = \frac{b}{2}\frac{p-1}{\sqrt{q^2 - (p-1)^2}}. \end{aligned} \tag{27}$$

In case $a > b$, η_1 and η_2 are both positive.

In case $\ell > a + b$, E has a cusp (ξ_S, η_S). The angle α_S associated with the cusp is determined from the condition that ξ_S is a stationary value. Equation (8) shows that with $\alpha = \alpha_S$, also $\ell_1 - \ell_2$ has a stationary value. The stationarity conditions

$$\left(\frac{\cos\beta}{\sin\alpha}\right)^k = \text{Max!} \quad (k = 1, 3) \tag{28}$$

result in the quadratic equation

$$\cos^2\alpha_S - \frac{p^2 + q^2 - 1}{pq}\cos\alpha_S = -1. \tag{29}$$

Stationary values exist if $|(p^2 + q^2 - 1)/(2pq)| > 1$. Equation (12) shows that this is the condition $\ell > a + b$. The line α_S is tangent to both branches of E.

By the lines $\alpha = \alpha_{\min}$ and $\alpha = \alpha_{\max}$ and by the curve E the ξ, η-plane is divided into domains differing in the *number of lines α on which every point of the domain* is located. Depending on the parameters a, b, ℓ, there are domains with numbers $k = 0$, 1, 2 or 3. If the body center of mass C is located on $k > 0$ lines $\alpha_1, \ldots, \alpha_k$, then the body has the equilibrium positions $\alpha_1, \ldots \alpha_k$. The parameters (c, γ) and (c', γ') (γ and γ' both positive and negative) determine four centers of mass C_1, C_2, C_3, C_4 which, in general, are located in different domains associated with different numbers k of equilibrium positions. For a graphical representation, see Fig. 3, based on Example 1.

Example 1 Given are the parameters $a = 6$, $b = 18$, $\ell = 28 > a + b$.
Equation (12) determines the extremal angles: $\cos\alpha_{\min} = 6/7$, $\alpha_{\min} \approx 31.00°$ and $\cos\alpha_{\max} = -3/7$, $\alpha_{\max} \approx 115.38°$. Figure 3 shows lines α for various angles $\alpha_{\min} \le \alpha \le \alpha_{\max}$ and the curve E enveloped by the manifold of lines. The data associated with E are: $\cos\alpha_0 \approx -0.2409$, $\xi_0/b = 1/2 - e_{2\min}/b \approx 0.1238$, $\eta_1/b = 3/\sqrt{13} \approx 0.8321$, $\eta_2/b = -3/\sqrt{160} \approx -0.2372$, $\cos\alpha_S = (31 - 2\sqrt{130})/21$, $\alpha_S \approx 67.03°$, $\xi_S/b \approx 0.3664$, $\eta_S/b \approx 0.1076$, $(\ell_1 - \ell_2)_{\max}/b \approx 1.045$.

By the curve E and the η-axis, the domain Γ_3 is defined every point of which is the point of intersection of three lines $\alpha_1, \alpha_2, \alpha_3$. Through points outside of Γ_3, a single line α is passing. This means three equilibrium positions $\alpha_1, \alpha_2, \alpha_3$ exist if the center of mass C is located in Γ_3. A single equilibrium position α exists if C is located outside of Γ_3. A shift of the center of mass from outside to inside of Γ_3 results in the bifurcation from one to three equilibrium positions. The total number n of equilibrium positions for four centers of mass C_1, C_2, C_3, C_4 is $4 \le n \le 8$ if $p < 1$ and $4 \le n \le 6$ if $p > 1$.

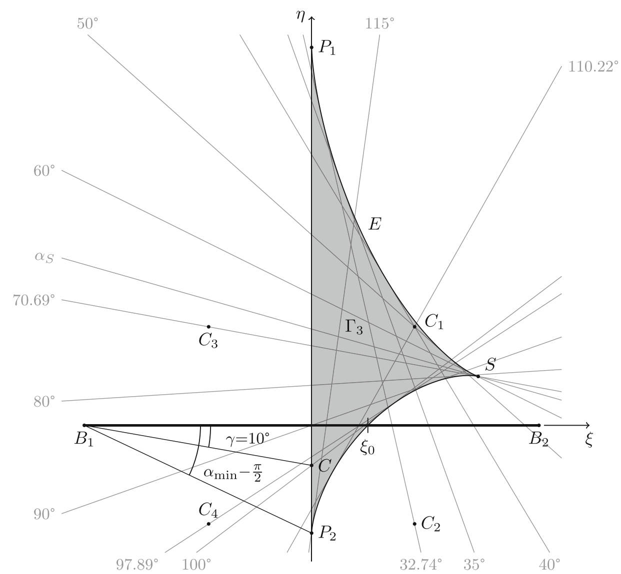

Fig. 3 Lines α, curve E, domain Γ_3, centers of mass C_1, C_2, C_3, C_4 for the data in Example 1. Center of mass C on the η-axis and associated angles γ and α in Sect. 4

To be specific, let C_1 be the point of intersection of the lines $\alpha_1 = 40°$ and $\alpha_2 = 50°$. It is located in Γ_3 very close to E. C_2, C_3, C_4 are located outside of Γ_3. From (21), the parameters $c \approx 13.64$, $\gamma \approx -16.63°$, $\mu \approx 0.4527$, $\sigma \approx -0.4339$ are calculated. With these parameters, (17) and (20) determine for the altogether six equilibrium positions the following parameters.

$C_1 : \alpha_1 = 40°$, $\ell_1 \approx 21.19$, $\ell_2 \approx 6.82$, $y_C \approx 10.30$ unstable ($y_C'' > 0$)
$C_1 : \alpha_2 = 50°$, $\ell_1 \approx 22.76$, $\ell_2 \approx 5.24$, $y_C \approx 10.30$ unstable ($\beta < 0$)
$C_1 : \alpha_3 \approx 110.22°$, $\ell_1 \approx 18.72$, $\ell_2 \approx 9.28$, $y_C \approx 7.73$ unstable ($y_C'' > 0, \beta < 0$)
$C_2 : \alpha_4 \approx 32.74°$, $\ell_1 \approx 17.69$, $\ell_2 \approx 10.31$, $y_C \approx 2.86$ unstable ($y_C'' > 0, \beta < 0$)
$C_3 : \alpha_5 \approx 70.69°$, $\ell_1 \approx 23.38$, $\ell_2 \approx 4.62$, $y_C \approx 17.93$ unstable ($\beta < 0$)
$C_4 : \alpha_6 \approx 97.89°$, $\ell_1 \approx 21.60$, $\ell_2 \approx 6.40$, $y_C \approx 19.42$ stable (y_C is the global maximum)

For the statements about stability and instability, see Sect. 6. In Fig. 4, the body is shown in all six positions. The unstable equilibrium positions α_1 and α_2 disappear when C_1 is shifted across the curve E.

Example 2 Given are the parameters $a = 6$, $b = 18$, $\ell = 20 < a + b$.

The extremal angles (12) are $\cos\alpha_{\min} = 7/15$, $\alpha_{\min} \approx 62.18°$ and $\cos\alpha_{\max} = -3/5$, $\alpha_{\max} \approx 126.87°$. Figure 3 is replaced by Fig. 5. The data associated with the curve E are: $\cos\alpha_0 \approx -0.3532$, $\xi_0/b \approx 0.1789$, $\xi_1/b = q^2/2 = 50/81 \approx 0.6173$, $\eta_1/b = (317/7128)\sqrt{11} \approx 0.1475$, $\eta_2/b = -3/8$. The domain above the line $\alpha_{\min}$ is the domain $x < 0$ in Fig. 2b. If the center of mass C is located in this domain, an equilibrium position with contact $B_2 = A_2$ exists. For this reason, this domain is denoted Γ_c with index c for contact. The number of equilibrium positions without contact is either zero or one or two depending upon whether C is located in the domains Γ_0, Γ_1 or Γ_2. The total number n of equilibrium conditions for four centers of mass C_1, C_2, C_3, C_4 is $2 \le n \le 6$.
To be specific, let C_1 be the point on the line $\alpha = 120°$ with the coordinates $\xi/b = 5\sqrt{17}/64 \approx 0.3231$, $\eta/b = (15 - 4\sqrt{3})/24 \approx 0.3363$ satisfying Eq. (21). These coordinates determine the parameters $c \approx 15.99$, $\gamma \approx -22.25°$, $\mu \approx 0.6441$, $\sigma \approx -0.6726$. C_1 and C_3 are located in Γ_c, C_2 and C_3 in Γ_0 and C_4 in Γ_1. The altogether four equilibrium positions are characterized by the following parameters.

$C_1 : \alpha_1 = 120°$, $\ell_1 \approx 14.76$, $\ell_2 \approx 5.24$, $y_C \approx 0.62$ unstable ($y_C'' > 0, \gamma' < 0$)
$C_2 : \alpha_2 = \alpha_{\min}$, $\ell_1 = 20$, $\ell_2 = 0$, unstable (contact at A_2, $\beta < 0$)
$C_3 : \alpha_3 = \alpha_{\min}$, $\ell_1 = 20$, $\ell_2 = 0$, unstable (contact at A_2, $\beta < 0$)
$C_4 : \alpha_4 \approx 102.49°$, $\ell_1 \approx 17.55$, $\ell_2 \approx 2.45$, $y_C \approx 17.98$ stable (y_C is absolute maximum)

For the statements about stability and instability, see Sect. 6. In Fig. 6, all four equilibrium positions are shown.

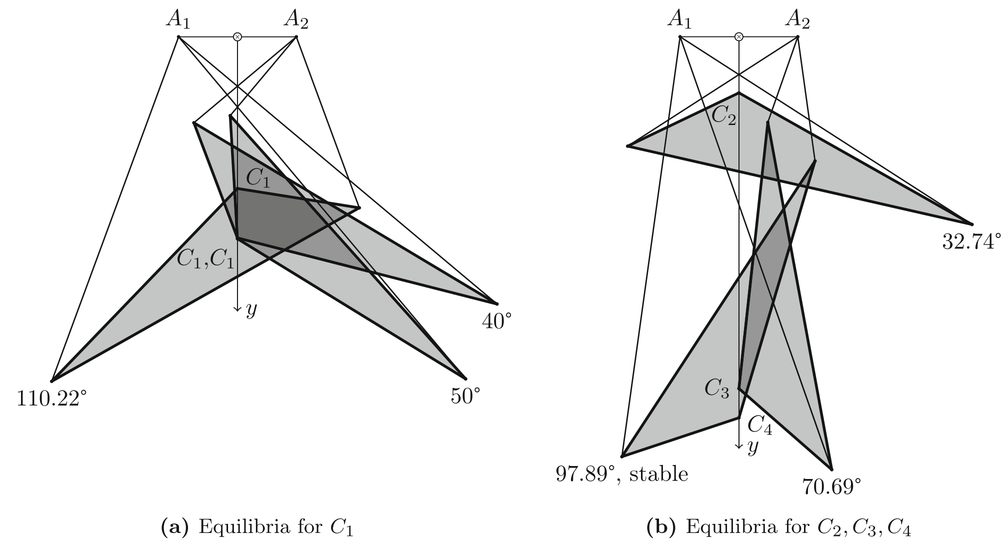

Fig. 4 Six equilibrium positions $\ell_1 > \ell_2 > 0$ of Example 1

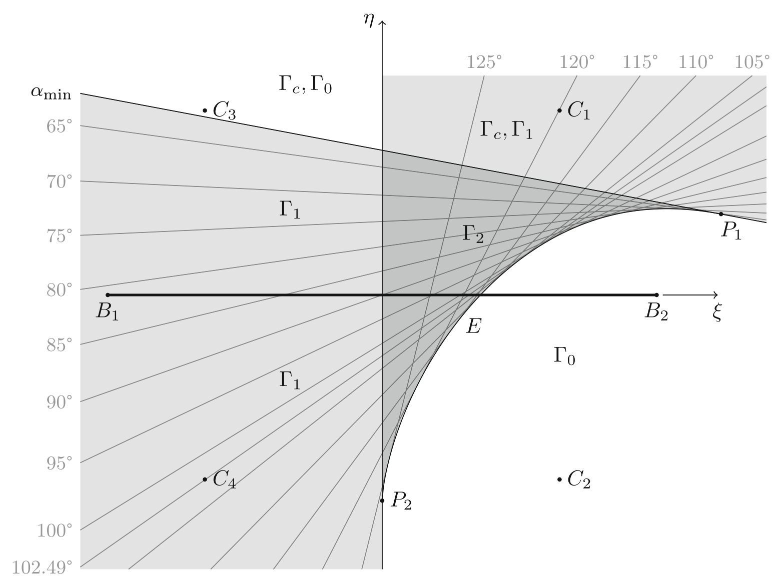

Fig. 5 Lines α, curve E, domains Γ_c, Γ_0, Γ_1, Γ_2, centers of mass C_1, C_2, C_3, C_4 for the data in Example 2

4 The symmetric body

The center of mass C of a symmetric body is located on the η-axis at the point $\eta = -(b/2)\tan\gamma$ (see Fig. 3). Only the case $\gamma \geq 0$ is considered because equilibrium positions with $\gamma < 0$ are unstable (see Sect. 6). Figure 3 shows that independent of γ, C is located on the line $\alpha_{\max}$. In the case $\eta_C > \eta_2$, C is also located on a second line $\alpha < \alpha_{\max}$. Hence, P_2 is a point of bifurcation. These results are in accordance with the equilibrium condition (17). For the symmetric body, Eq. (15) yields $\mu = 0$, $\sigma = \tan\gamma$. Hence, the equilibrium condition reads

$$(\cot\alpha + \tan\gamma)\cos\beta = 0. \tag{30}$$

The solution $\cos\beta = 0$ determines, independent of γ, the equilibrium position $\alpha = \alpha_{\max}$. The solution

$$\cot\alpha = -\tan\gamma \quad \text{or} \quad \gamma = \alpha - \pi/2 \tag{31}$$

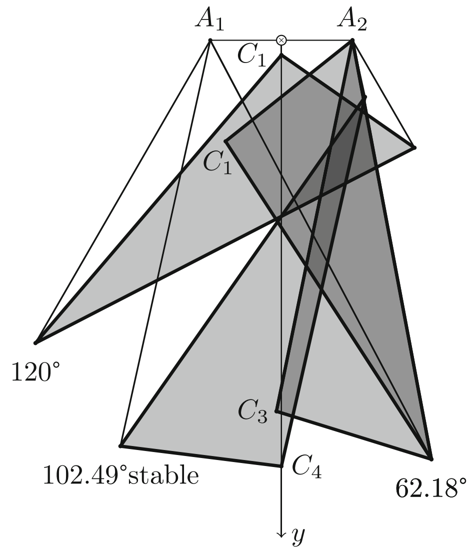

Fig. 6 Four equilibrium positions $\ell_1 > \ell_2 \geq 0$ of Example 2

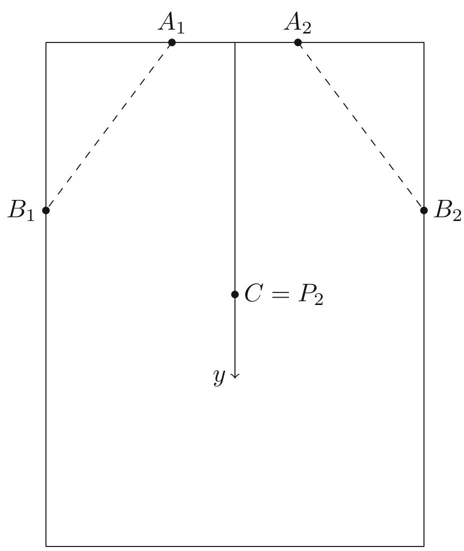

Fig. 7 Rectangular frame suspended

determines an additional tilted equilibrium position. It exists only for angles $0 \leq \gamma \leq \alpha_{\max} - \pi/2$. In Fig. 3, the relationship between γ and α is illustrated by the angles $(\gamma = \alpha_{\max} - \pi/2, \alpha = \alpha_{\max})$, $(\gamma = 10°, \alpha = 100°)$ and $(\gamma = 0, \alpha = \pi/2)$. From Eq. (26), it is known that $\eta_2 > 0$ if $a > b$. In this case, no bifurcation occurs if $\gamma \geq 0$. Stability criteria see in Sect. 6.

Example 3 A rectangular picture frame (width b, height h, center of mass C = geometric center) is to be suspended with parameter $p < 1$ such that (i) A_1, A_2 and B_1, B_2 are on the circumference and (ii) C is the point of bifurcation P_2 (Fig. 7). Under which condition on $\lambda = h/b$ is this suspension possible?

Solution: $y_C = h/2$ and $y_C = (\ell/2)\sin\alpha_{\max} - \eta_2$. With Eq. (12) and (26), this yields the equation

$$\lambda = \sqrt{q^2 - (p-1)^2} - \frac{p-1}{\sqrt{q^2 - (p-1)^2}} \tag{32}$$

or, resolved for q^2,

$$q^2 = p(p-1) + \frac{\lambda}{2}[\lambda + \sqrt{\lambda^2 + 4(p-1)}]. \tag{33}$$

The condition on λ is $\lambda^2 \geq 4(1-p)$. Under this condition, $q^2 \geq (1-p)(2-p)$.

5 The single-hook suspension ($a = 0$)

Results for this case were obtained in [19]. Equation (19) yields $v = w = q$. With this, Eq. (20) becomes

$$[2\mu q u(u^2-1)]^2 = (u^2 \pm 2\sigma u - 1)^2\,[(1+u^2)^2 - q^2(u^2-1)^2]. \tag{34}$$

Equations (3), (12) and (21) – (29) yield $q > 1$, $\cos\alpha_{\min} = 1/q\ \cos\alpha_{\max} = -1/q$, $\eta_{1,2} = \pm(b/2)/\sqrt{q^2-1}$, $\cos\alpha_S = 0$, $\xi_S = b/(2q)$ and $\eta_S = 0$. The curve E is symmetric with respect to the ξ-axis. Equation (6) yields

$$q = -\frac{\sin\beta}{\cos\alpha}, \qquad \sqrt{q^2-1} = \frac{\sqrt{\sin^2\alpha - \cos^2\beta}}{\sin\alpha}. \tag{35}$$

With this, Eqs. (21) and (23) yield

$$2q\frac{\xi}{b} = \left(\frac{\cos\beta}{\sin\alpha}\right)^3, \qquad 2\sqrt{q^2-1}\,\frac{\eta}{b} = \frac{(\sin^2\alpha - \cos^2\beta)^{3/2}}{\sin^3\alpha} \tag{36}$$

and, consequently,

$$\left(2q\frac{\xi}{b}\right)^{2/3} + \left(2\sqrt{q^2-1}\,\frac{\eta}{b}\right)^{2/3} = 1, \tag{37}$$

which is the equation of the astroid. Thus, the curve E is a projection of the astroid. In [19], these results were obtained by a different method.

6 Stability, instability

Among several equilibrium positions, the position with the maximum y_C is stable. By this criterion, the position α_6 in Example 1 and the position α_4 in Example 2 are stable.

From (7) and (16), it follows that

$$\left.\begin{aligned} y_C' &= \frac{\mathrm{d}y_C}{\mathrm{d}\alpha} = \frac{\ell}{2}\frac{\sin\alpha}{\cos\beta}[\mu\sin\beta + (\cot\alpha + \sigma)\cos\beta], \\ y_C'' &= \frac{\mathrm{d}^2 y_C}{\mathrm{d}\alpha^2} = \frac{\ell}{2}\left[-\sin\alpha + \sigma\cos\alpha + \mu\left(q\frac{\sin^2\alpha}{\cos^3\beta} + \cos\alpha\tan\beta\right)\right]. \end{aligned}\right\} \tag{38}$$

$y_C' = 0$ in equilibrium positions. An equilibrium position is unstable if $y_C'' > 0$. By this criterion, the positions $\alpha_1, \alpha_3, \alpha_4$ in Example 1 and the position α_1 in Example 2 are unstable.

Theorem 1 *An equilibrium position with contact $B_2 = A_2$ is stable if and only if*

$$\beta > \gamma' > 0. \tag{39}$$

Proof The system in Fig. 2b with contact $B_2 = A_2$ has two degrees of freedom. The triangle B_1, B_2, C is rotated through the angle φ about the unit vector $\vec{n}_1$ with coordinates $[n_x, n_y, 0] = [-\sin\beta, \cos\beta, 0]$. Following this first rotation, the entire system is rotated by the angle ψ around the unit vector $\vec{n}_2$, which has coordinates $[1, 0, 0]$. After the first rotation, the vector $\vec{r} = \overrightarrow{B_2C}$ is in the position

$$\vec{r}^{\,*} = \cos\varphi\,\vec{r} + (1-\cos\varphi)(\vec{n}_1\cdot\vec{r})\vec{n}_1 + \sin\varphi\,\vec{n}_1\times\vec{r} \tag{40}$$

with $\vec{n}_1\cdot\vec{r} = n_x r_x + n_y r_y = c'\cos\gamma'$. The vector $\vec{n}_1\times\vec{r}$ is directed along the negative z-axis, and the z-coordinate is $-n_y r_x + n_x r_y = -c'\sin\gamma'$.

The second rotation carries the vector $\vec{r}^{\,*}$ into the position

$$\vec{r}^{\,**} = \cos\psi\,\vec{r}^{\,*} + (1-\cos\psi)(\vec{n}_2\cdot\vec{r}^{\,*})\vec{n}_2 + \sin\psi\,\vec{n}_2\times\vec{r}^{\,*}. \tag{41}$$

The coordinate y_C of the center of mass is the y-coordinate of $\vec{r}^{\,**}$:

$$y_C = r_y^* \cos\psi - r_z^* \sin\psi. \tag{42}$$

Equation (40) yields

$$\left.\begin{aligned} r_y^* &= \cos\varphi\, r_y + (1-\cos\varphi)(n_x r_x + n_y r_y) n_y \;= \cos\varphi [r_y(1-n_y^2) - r_x n_x n_y] + (\vec{n}_1 \cdot \vec{r}) n_y \\ &= \cos\varphi\, n_x (r_y n_x - r_x n_y) + \cos\beta\, c' \cos\gamma' = \cos\varphi \sin\beta\, c' \sin\gamma' + c' \cos\gamma' \cos\beta, \\ r_z^* &= -\sin\varphi\, c' \sin\gamma'. \end{aligned}\right\} \tag{43}$$

Hence,

$$y_C = c'[\cos\psi(\cos\varphi \sin\beta \sin\gamma' + \cos\beta\cos\gamma') + \sin\psi \sin\varphi \sin\gamma']. \tag{44}$$

This yields (omitting the factor c')

$$\left.\frac{\partial^2 y_C}{\partial\varphi^2}\right|_{(0,0)} = -\sin\beta\sin\gamma', \qquad \left.\frac{\partial^2 y_C}{\partial\psi^2}\right|_{(0,0)} = -\cos(\beta-\gamma'), \qquad \left.\frac{\partial^2 y_C}{\partial\varphi\partial\psi}\right|_{(0,0)} = -\sin\gamma'. \tag{45}$$

Stability requires that two conditions are satisfied:

$$\begin{aligned} &\text{(a)}\ -\sin\beta\sin\gamma' < 0, \\ &\text{(b)} \begin{vmatrix} -\sin\beta\sin\gamma' & -\sin\gamma' \\ -\sin\gamma' & -\cos(\beta-\gamma') \end{vmatrix} = \cos\beta\sin\gamma'\sin(\beta-\gamma') > 0. \end{aligned} \tag{46}$$

Both conditions are satisfied if and only if $\beta > \gamma' > 0$. □

By this theorem, the position shown in Fig. 2b is stable, and the two positions $\alpha = \alpha_{\min}$ in Example 2 are unstable.

Theorem 2 *An equilibrium position with $\ell_1 \geq \ell_2 > 0$ is unstable if the condition $\beta > \gamma' > 0$ is violated.*

Proof In the equilibrium position under investigation, the quadrilateral $A_1 - B_1 - B_2 - A_2$ is considered rigid. The resulting system has two degrees of freedom. If this system is unstable, the system with five degrees of freedom is also unstable. Repetition of the arguments in the proof of Theorem 1 leads to Theorem 2. □

By this theorem, the positions $\alpha_2, \alpha_3, \alpha_4, \alpha_5$ in Example 1 and the position α_1 in Example 2 are unstable.

Next, the equilibrium positions of the symmetric body, described in Sect. 4, are investigated. The single equilibrium position $\alpha = \alpha_{\max}$ existing in the case $\gamma \geq \alpha_{\max} - \pi/2$ is stable.

Theorem 3 *In the case $0 \leq \gamma < \alpha_{max} - \pi/2$, the equilibrium position $\alpha = \alpha_{max}$ (position 1) is unstable, whereas the tilted equilibrium position $\cot\alpha = -\tan\gamma$ (position 2) is stable.*

Proof The position with the larger (the smaller) coordinate y_C is stable (unstable). Hence, it must be shown that y_{C2} (position 2) is larger than y_{C1} (position 1). Equation (16) yields

$$y_{C1} = \frac{b}{2}(q\sin\alpha_{\max} + \tan\gamma), \qquad y_{C2} = \frac{b}{2}(q\sin\alpha + \tan\gamma\sin\beta). \tag{47}$$

With $\tan\gamma = -\cot\alpha$, $\sin\beta = p - q\cos\alpha$ and $\cos\alpha_{\max} = (p-1)/q$

$$\begin{aligned} y_{C2} - y_{C1} &= \frac{b}{2}\left[q(\sin\alpha - \sin\alpha_{\max}) - \frac{\cos\alpha}{\sin\alpha}(p - q\cos\alpha - 1)\right] \\ &= \frac{b}{2}\frac{q}{\sin\alpha}\left[1 - \sin\alpha\sin\alpha_{\max} - \cos\alpha\frac{p-1}{q}\right] \\ &= \frac{\ell}{2\sin\alpha}[1 - \cos(\alpha_{\max} - \alpha)] > 0. \end{aligned} \tag{48}$$

□

Suspension II

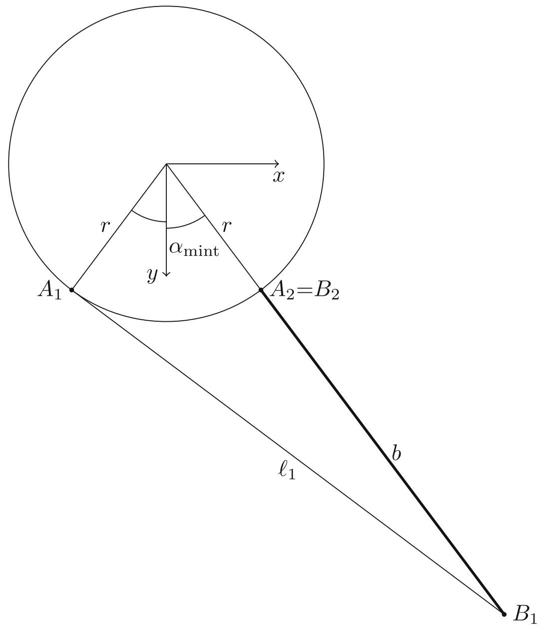

Fig. 8 Contact $B_2 = A_2$ with $q = q_t$, $\alpha_{\min} = \alpha_{\text{mint}}$

7 Equilibrium positions

The arguments in Sect. 3 are valid also for Fig. 1b. In a state of (stable or unstable) equilibrium with $\ell_1, \ell_2 \neq 0$ the straight sections $A_1 - B_1$ and $A_2 - B_2$ of the string are under the same angle $\alpha > 0$ against the horizontal x-axis. Hence, the

$$\text{equilibrium condition} \quad x_C = 0 \quad (\ell_{1,2} \neq 0). \tag{49}$$

The total length of the string is $L = \ell_1 + \ell_2 + 2r(\pi - \alpha)$. With the constant length $\ell = L - 2\pi r$,

$$\ell = \ell_1 + \ell_2 - 2r\alpha. \tag{50}$$

$$\text{Def:} \quad p = 2r/b, \quad q = \ell/b \tag{51}$$

For the reasons given in Sect. 3, equilibrium positions with $\ell_1 \geq \ell_2$ are determined for the four parameter combinations $(c, \pm\gamma)$ and $(c', \pm\gamma')$.

Equations (5)–(10) are replaced by:

$$B_1 = [-r \sin\alpha + \ell_1 \cos\alpha \ , \ r\cos\alpha + \ell_1 \sin\alpha], \qquad B_2 = [r\sin\alpha - \ell_2 \cos\alpha \ , \ r\cos\alpha + \ell_2 \sin\alpha]. \tag{52}$$

$$\sin\beta = (x_{B_2} - x_{B_1})/b = p\sin\alpha - (q + p\alpha)\cos\alpha, \tag{53}$$

$$\frac{\mathrm{d}}{\mathrm{d}\alpha}\sin\beta = (q + p\alpha)\sin\alpha, \quad \frac{\mathrm{d}}{\mathrm{d}\alpha}\cos\beta = -(q + p\alpha)\sin\alpha\tan\beta, \quad \frac{\mathrm{d}}{\mathrm{d}\alpha}\tan\beta = (q + p\alpha)\frac{\sin\alpha}{\cos^3\beta}. \tag{54}$$

$$\ell_1 - \ell_2 = b\frac{\cos\beta}{\sin\alpha}, \quad \ell_{1,2} = \frac{b}{2}\left(q + p\alpha \pm \frac{\cos\beta}{\sin\alpha}\right), \quad e_{1,2} = \frac{\mp x_{B_{1,2}}}{\sin\beta} = \frac{b}{2}(1 \mp \cot\alpha\cot\beta). \tag{55}$$

Extremal angles $\alpha_{\min}$ and $\alpha_{\max}$ occur in the positions with $\sin\beta = -1$ and $\sin\beta = +1$, respectively:

$$p\sin\alpha - (q + p\alpha)\cos\alpha = \begin{cases} -1 \ (\alpha = \alpha_{\min}) \\ +1 \ (\alpha = \alpha_{\max}). \end{cases} \tag{56}$$

The formula for $\alpha_{\min}$ does not apply if the parameters p and q allow a position with contact $B_2 = A_2$. Let q_t be the largest q allowing contact. q_t and the associated α_{mint} are obtained from Fig. 8:

$$\frac{\ell_1}{b} = \sqrt{1+p}, \quad \sin 2\alpha_{\text{mint}} = \frac{2\sqrt{1+p}}{2+p}, \quad q_t = \sqrt{1+p} - p\,\alpha_{\text{mint}}. \tag{57}$$

In the case $q < q_t$, α_{min} is larger than α_{mint}. The relationship between q and α_{min} is obtained from the contact condition $\ell_2 = 0$, $(q + p\alpha_{\text{min}})\sin\alpha_{\text{min}} = \cos\beta$, whence it follows from (53) that

$$q = \frac{p}{2}(\sin 2\alpha_{\text{min}} - 2\alpha_{\text{min}}) + \sqrt{1 - p^2 \sin^4 \alpha_{\text{min}}}. \tag{58}$$

Example $p = 1/3$ yields $q_t \approx 0.9168$, $\alpha_{\text{mint}} \approx 40.89°$. With $p = 1/3$ and $\alpha_{\text{min}} = 45°$, Eq. (58) yields $q \approx 0.8909 < q_t$.

The equilibrium condition (13) is valid also for suspension II:

$$\text{The position with contact } B_2 = A_2 \text{ is an equilibrium position if in this position } x_C \le 0. \tag{59}$$

7.1 Equilibrium positions with $\ell_1 \ge \ell_2 > 0$

Equation (17) is valid:

$$\mu \sin\beta + (\cot\alpha \pm \sigma)\cos\beta = 0, \qquad -\mu\sin\beta + (\cot\alpha \pm \sigma)\cos\beta = 0. \tag{60}$$

Without introducing extraneous roots, squaring results in the equations

$$\mu^2[p\sin\alpha - (q+p\alpha)\cos\alpha]^2 = (\cot\alpha \pm \sigma)^2\left\{1 - [p\sin\alpha - (q+p\alpha)\cos\alpha]^2\right\}. \tag{61}$$

Each solution $\alpha > 0$ of these two equations determines an equilibrium position.

7.2 Lines α

Equations (21)–(23) defining the lines α and the curve E are replaced by

$$F = -\frac{\eta}{b} + \frac{\xi}{b}\tan\beta + \frac{1}{2}\cot\alpha = 0, \qquad \frac{\mathrm{d}F}{\mathrm{d}\alpha} = \frac{\xi}{b}\,\frac{(q+p\alpha)\sin\alpha}{\cos^3\beta} - \frac{1}{2\sin^2\alpha} = 0, \tag{62}$$

$$\frac{\xi}{b} = \frac{1}{2(q+p\alpha)}\left(\frac{\cos\beta}{\sin\alpha}\right)^3, \tag{63}$$

Equations (25) and (26) are replaced by

$$[p\sin\alpha_0 - (q+p\alpha_0)\cos\alpha_0]\Big[1 - [p\sin\alpha_0 - (q+p\alpha_0)\cos\alpha_0]^2\Big] + (q+p\alpha_0)\cos\alpha_0\sin^2\alpha_0 = 0, \tag{64}$$

$$\eta_{1,2} = \frac{b}{2}\cot\alpha_{\text{min, max}}. \tag{65}$$

In the case $q > q_t$ (no contact $B_2 = A_2$), E has a cusp. The stationarity condition (28) is replaced by

$$\frac{1}{q+p\alpha}\left(\frac{\cos\beta}{\sin\alpha}\right)^3 = \text{Max!} \tag{66}$$

This results in the equation for the associated angle α_S

$$3(q+p\alpha_S)^2\sin^2\alpha_S\sin\beta + (4p\sin\alpha_S - 3\sin\beta)\cos^2\beta = 0. \tag{67}$$

Equation (38) for y_C'' is replaced by

$$y_C'' = \frac{b}{2}\left\{p\Big[\cos\alpha + (\mu\tan\beta \pm \sigma)\sin\alpha\Big] + (q+p\alpha)\Big[-\sin\alpha + (\mu\tan\beta \pm \sigma)\cos\alpha + \mu(q+p\alpha)\frac{\sin^2\alpha}{\cos^3\beta}\Big]\right\}. \tag{68}$$

8 Conclusion and scope for future research

This study analyzed the equilibrium positions and stability of a rigid body suspended by a massless, flexible, inextensible string in two setups: Suspension I, with two fixed frictionless hooks, and Suspension II, with a frictionless pulley. Equilibrium conditions were derived, and a bifurcation curve E was identified, marking changes in the number of equilibrium positions. Stability criteria and differences between the cases $a < b$ and $a > b$ were established, with special cases such as symmetric bodies and single-hook suspensions also analyzed.

The results highlight critical conditions for avoiding dangerous transitions relevant to safety-critical systems. Applications include setups where small perturbations may lead to sudden movements, such as suspended objects under changing loads or external forces.

Future work could model dry friction effects as discussed by *Burov* and *Nikonov* [20]. Dynamic factors, including micro-vibrations, wind, or precipitation, could be analyzed for suspended systems. External forces causing transitions between equilibrium positions are worth investigating, particularly for applications like floating cranes [11] or fluid-filled containers with dynamic loads [9,10]. Time-dependent parameter variations, such as moving suspension points or shifting loads, also present an interesting topic for further investigations. Finally, experimental validation could address influences like string elasticity or air resistance.

Acknowledgements The authors thank Clemens Kummer for converting the figures into digital form. We also acknowledge the use of Grammarly and Writefull for language editing purposes.

Open Access This article is licensed under a Creative Commons Attribution 4.0 International License, which permits use, sharing, adaptation, distribution and reproduction in any medium or format, as long as you give appropriate credit to the original author(s) and the source, provide a link to the Creative Commons licence, and indicate if changes were made. The images or other third party material in this article are included in the article's Creative Commons licence, unless indicated otherwise in a credit line to the material. If material is not included in the article's Creative Commons licence and your intended use is not permitted by statutory regulation or exceeds the permitted use, you will need to obtain permission directly from the copyright holder. To view a copy of this licence, visit http://creativecommons.org/licenses/by/4.0/.

Funding Open Access funding enabled and organized by Projekt DEAL. This research received no external funding. The authors acknowledge institutional support from the Karlsruhe Institute of Technology.

Declarations

Data availability No datasets were generated or analyzed during the current study.

Conflict of interest The authors have no relevant financial or non-financial interests to disclose.

References

1. Appell, P.: Traité de Mécanique Rationnelle. Tome I. Gauthier-Villars, Paris (1893)
2. Levi-Civita, T., Amaldi, U.: Lezioni di Meccanica Razionale, vol. 1. N. Zanichelli, Bologna, Italy (1923). (**Part 2**)
3. Rodnikov, A.V.: The algorithms for capture of the space garbage using "leier constraint". Reg. Chaot. Dyn. **11**(4), 483–489 (2006). https://doi.org/10.1070/RD2006v011n04ABEH000366
4. Rodnikov, A.V.: On the leier influence on a dumbbell motion in the central newtonian force field. Nelin. Dinam. **5**(4), 519–533 (2009). https://doi.org/10.20537/nd0904005
5. Rodnikov, A.V.: On a particle motion along the leier fixed in a precessing rigid body. Nelin. Dinam. **7**(2), 295–311 (2011). https://doi.org/10.20537/nd1102007
6. Rodnikov, A.V., Krasil'nikov, P.S.: On spacial motions of an orbital tethered system. Rus. J. Nonlin. Dyn. **13**(4), 505–518 (2017). https://doi.org/10.20537/nd1704004
7. Burov, A.A.: The existence and stability of the equilibria of mechanical systems with constraints produced by large potential forces. J. Appl. Math. Mech. **67**(2), 193–200 (2003). https://doi.org/10.1016/S0021-8928(03)90005-0
8. Ellermann, K., Kreuzer, E.J.: Nonlinear dynamics in the motion of floating cranes. Multibody Syst. Dyn. **9**, 377–387 (2003)
9. Trahan, R., Kalmar-Nagy, T.: Equilibrium, stability, and dynamics of rectangular liquid-filled vessels. J. Comput. Nonlinear Dyn. **6**, 041012 (2011). https://doi.org/10.1115/1.4003915
10. Sah, S.M., Mann, B.P.: Potential well metamorphosis of a pivoting fluid-filled container. Physica D **241**(19), 1660–1669 (2012). https://doi.org/10.1016/j.physd.2012.07.001
11. Erdös, P., Schibler, G., Herndon, R.C.: Floating equilibrium of symmetrical objects and the breaking of symmetry. part 1: Prisms. Am. J. Phys. **60**(4), 335–345 (1992). https://doi.org/10.1119/1.16877
12. Kobylinski, L., Kastner, S.: Stability and Safety of Ships: Regulation and Operation. Elsevier Ocean Engineering Series. Elsevier Science, Amsterdam (2003). https://books.google.de/books?id=KswLAAAACAAJ

13. Bailey, R.C.: Implications of iceberg dynamics for iceberg stability estimation. Cold Reg. Sci. Technol. **22**(2), 197–203 (1994). https://doi.org/10.1016/0165-232X(94)90028-0
14. Schorr, P., Böhm, V., Zentner, L., Zimmermann, K.: Motion characteristics of a vibration driven mobile tensegrity structure with multiple stable equilibrium states. J. Sound Vib. **437**, 198–208 (2018). https://doi.org/10.1016/j.jsv.2018.09.019
15. Poston, T., Stewart, I.: Catastrophe Theory and Its Applications. Dover books on mathematics. Dover Publications, Melbourne (1996). https://books.google.de/books?id=7Zm5zTh8rLAC
16. Poston, T., Woodcock, A.: Zeeman's catastrophe machine. Math. Proc. Cambridge Philos. Soc. **74**(2), 217–226 (1973). https://doi.org/10.1017/S0305004100048003
17. Arnold, V.I.: Catastrophe Theory, 3rd edn. Springer Book Archive, p. 150. Springer, Steklov Mathematical Institute, Moscow, Russia (1992). https://doi.org/10.1007/978-3-642-58124-3
18. Stépán, G., Bianchi, G.: Stability of hanging blocks. Mech. Mach. Theory **29**(6), 813–817 (1994). https://doi.org/10.1016/0094-114X(94)90080-9
19. Genda, A., Stepan, G.: On the stability of bodies suspended asymmetrically with an inelastic rope. Acta Mech. **234**, 3009–3018 (2023). https://doi.org/10.1007/s00707-023-03546-x
20. Burov, A.A., Nikonov, V.I.: On the equilibria of a heavy hoop suspended on a nail. Mech. Solids **59**, 11–19 (2024). https://doi.org/10.1134/S0025654423601106

Publisher's Note Springer Nature remains neutral with regard to jurisdictional claims in published maps and institutional affiliations.